Hindawi
Shock and Vibration
Volume 2021, Article ID 6985661, 13 pages
https://doi.org/10.1155/2021/6985661

Research Article

PZT Actuators' Effect on Vibration Control of the PRRRP 2-DOF Flexible Parallel Manipulator

Amin Valizadeh [1] **and Morteza Shariatee** [2]

[1]*Department of Mechanical Engineering, Ferdowsi University of Mashhad, Mashhad, Iran*
[2]*Department of Mechanical Engineering, Iowa State University, Ames, IA, USA*

Correspondence should be addressed to Amin Valizadeh; amin.valizadeh@mail.um.ac.ir

Received 14 April 2021; Revised 21 June 2021; Accepted 1 July 2021; Published 10 July 2021

Academic Editor: Claudio Sbarufatti

Thanks to their advantages over rigid ones, interest for lightweight parallel manipulator was increased. Besides, structural flexibility effects at high operational speeds are more significant. Thus, developing an appropriate model for the assessment of the dynamic properties of flexible mechanisms and linkages to gain effective vibration control will raise high demand. Therefore, this paper represents the dynamic and kinematic modeling using the assumed mode method and first-type Lagrange equations of the 2-DOF planar parallel manipulator with two flexible links. To truly predict vibrations of the manipulator without any major simplifying assumptions, nonlinear dynamic modeling, which thoroughly attempts to represent the flexible behavior of the links, is considered. As a result, an active damping approach is being studied with PZT actuators. The results show that this approach is effective in damping the vibrations of the links that give accurate trajectory control.

1. Introduction

With regard to parallel manipulators with a lightweight structure, a planar parallel manipulator with lightweight linkages provides a high-speed alternative positioning mechanism for manipulators of serial architecture. These robots are used in a wide range of applications, from simple selection and location of robotic systems for industrial applications to microsurgical applications, maintenance of nuclear power plants, or space robotics [1]. The interest in research into flexible connection manipulators and mechanisms was significantly increased to make full use of the potential offered by flexible manipulators. It is, nevertheless, particularly challenging to control flexible manipulators so that precise positioning can be maintained. For a two-link flexible manipulator, the problem becomes more complex. The dynamics are highly nonlinear and complex due to the flexibility of the system [2, 3]. Although lightweight links are more likely to meet high-speed and high-acceleration requirements, the inertia and forces from the actuators are more likely than ever to deflect and vibrate [4]. The structural flexibility effects at high end-effector speeds are much more significant. Manipulators and mechanisms with flexible links are systems with a variety of degrees of freedom. They are described by coupled nonlinear partial differential equations of motion. The dynamic model formulation of manipulators with flexible links and mechanisms was based on different discretization ways of flexible links to devise and apply a real-time controller for joint movements and vibration removal. The most popular approaches are the finite element method (FEM) [5, 6] and the assumed mode method (AMM) [7, 8]. It has been commonly established to model a flexible single link manipulator. Various approaches were developed, mainly divisible into two categories: the approach to numerical analysis and the assumed method mode (AMM) [9, 10]. AMM examines approximate models by solving a partial differential equation that characterizes the system's dynamic behavior.

Previous studies have been reported using this approach to model a flexible single-link manipulator [11, 12]. Zhou

et al. recently developed dynamic equations for a flexible three-PRS manipulator with regard to vibrational analyses using the FEM method [13], taking into consideration link flexibility. Kang and Mills introduced a dynamic flexible-link 3-PRR planar parallel manipulator by employing AMM [14]. The existing parallel 2-DOF manipulator with solid links for an optimal design was studied [7]. In high-speed pick-and-place applications, this manipulator is also productive [15]. Nevertheless, no research has been conducted on the dynamic modeling of the mechanism, taking into account the flexibility in which industrial operations are inevitable. This paper considers a method of active damping using piezoelectric materials. Deformation of the flexible links produces shear stress that PZT materials can counteract due to the voltage control applied. PZT can achieve better performance in vibration damping than other transducer materials as PZT has higher stress constant [16–19].

Due to the promising results, the parallel kinematic machine (PKM) is the greatest increasing need of the machining and pick and place industry. Due to their high structural stiffness and rigidity, PKMs' absolute positioning error is reduced. The 2-DOF PRRRP PKM machine tool proves to achieve competing accuracies in the end tool [15]. However, the heavy and bulky links used to give adequate stiffness and accuracy significantly increase equipment costs, motor torques (power), and energy consumption. To overcome this issue, as a real-world requirement, research on the use of lightweight robot links is carried out in this paper. To overcome the positioning error due to the flexibility of the links, an active vibration control system based on PZT actuators is implemented.

In the present paper, an AMM modeling of the flexible links following Lagrangian method and a PD feedback control with linear velocity feedback (L-type) is used to correctly attenuate vibration due to trajectory tracking. This is followed by a proper PD trajectory control. The proposed active vibration damping approach was verified by simulations for flexible linkage manipulators.

2. Kinematic Modeling

Figure 1 illustrates the planar 2-DOF parallel manipulator with two flexible links. The manipulator architecture is 2-PRRRP, while R and P represent revolute and prismatic joints, respectively. In a plane that works properly for pick and place tasks, the end-effector offers high precision 2-DOF translational motion. The end-effector position vector, two active prism joints, and two passive revolute joints are presented as follows, respectively, about the fixed X-y reference framework displayed in Figure 2:

$$\begin{aligned} \overline{X}_e &= [\, x \;\; y \,]^T, \\ \overline{q} &= [\, q_1 \;\; q_2 \,]^T, \\ \overline{\beta} &= [\, \beta_1 \;\; \beta_2 \,]^T. \end{aligned} \tag{1}$$

As a deformation assumption and design criteria of the flexible links, the influence of transverse, shear, and rotary inertia has not been taken into account since the beam is long and slender. Links only vibrate horizontally, and the torsion and vertical bending are not considered. Besides, the beam properties variation can be neglected across the whole body and cross section [20].

Consequently, Euler–Bernoulli beam theory can be employed to simulate the manipulator's elastic behavior. The product of position-and time-dependent functions, i.e., AMM, expresses the deflection of the link, w_i, as

$$w_i(x,t) = \sum_{j=1}^{r} \eta_{ij}(t)\varphi_j(\xi). \tag{2}$$

In the equation above, $\xi = x/l$, j and r denote the jth vibration mode and a finite number of assumed modes, respectively.

To select the boundary conditions, one can take many different approaches in the AMM. The optimum set is found closest to the system's natural modes among the hypothesized modes in ideal situations. Thus, no assumption can be made about the employed set of hypothesized modes since several structural factors of the manipulator determine the natural modes [21]. In this study, pin-free modeling, implemented in a flexible PKM [16, 19], is considered for boundary conditions, which causes a significant deflection in the flexible links and remarkably investigates the effect of PZT actuators on damping the vibrations of flexible links. The alternative in the future needs an evaluation based on the robot's actual structure to improve outcomes in the results.

Given the boundary conditions of the flexible links on S_i and the end-effector, the selected normalized shape function that satisfies a pin-free boundary condition is as follows:

$$\varphi_j(\xi) = \frac{1}{2\,\sin(\gamma_j)} \times \left[\sin(\gamma_j \xi) + \frac{\sin(\gamma_j)}{\sinh(\gamma_j)} \sinh(\gamma_j \xi) \right], \tag{3}$$

where

$$\begin{aligned} &0 \le \xi \le 1, \\ &\gamma_j = (j + 0.25)\pi. \end{aligned} \tag{4}$$

The shape functions in the first three mode shapes of the flexible link are shown in Figure 3. The inverse kinematics problem is solvable by expanding the following restrictive equation, as shown in Figure 2:

$$OE = OA_i + q_i + b_i + w_i(l), \quad i = 1, 2, \tag{5}$$

which yields

$$\begin{cases} q_1 = \pm\sqrt{L^2 - (x-d)^2 + w_1^2(l)} + y, \\ q_2 = \pm\sqrt{L^2 - (x+d)^2 + w_2^2(l)} + y. \end{cases} \tag{6}$$

Equation (6) states that four solutions are available for the inverse kinematics of the mechanism. The four alternatives are consistent with four types of mechanism work modes. The deflection term, i.e., w_i, should be drawn from dynamic modeling to approach the solutions.

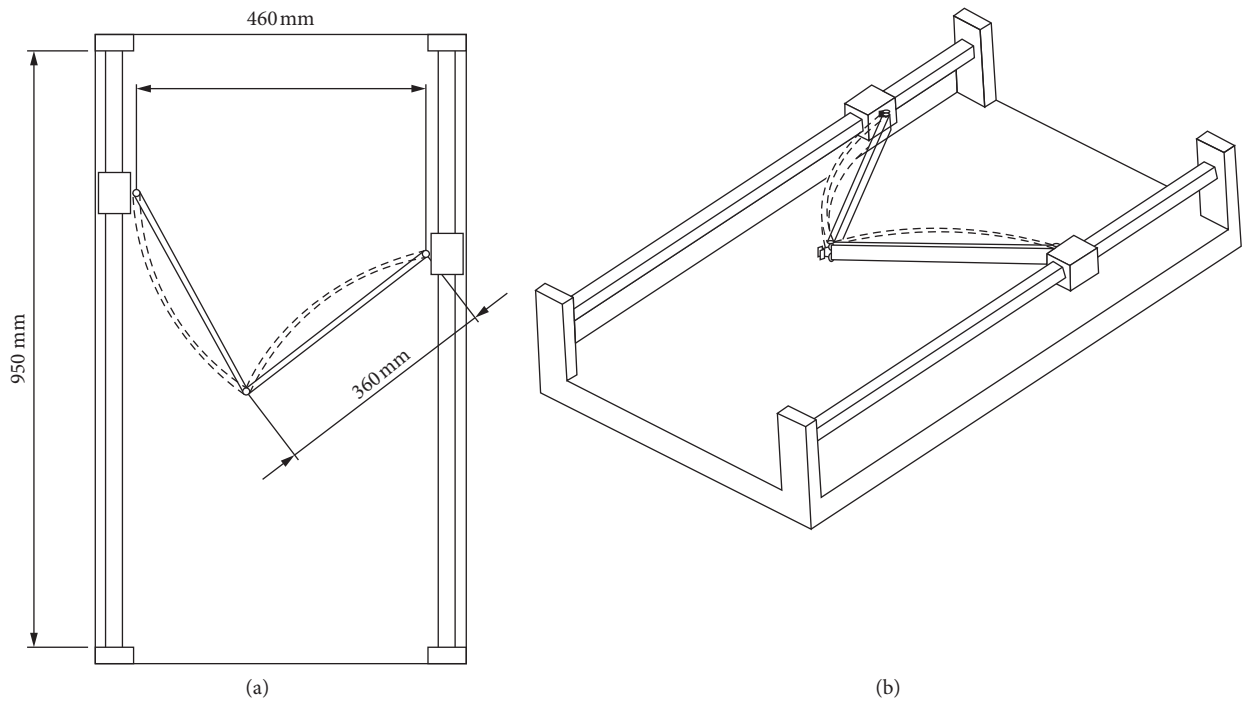

Figure 1: Architecture of 2-PRRRP with flexible links (dashed lines denote the deflection of the links).

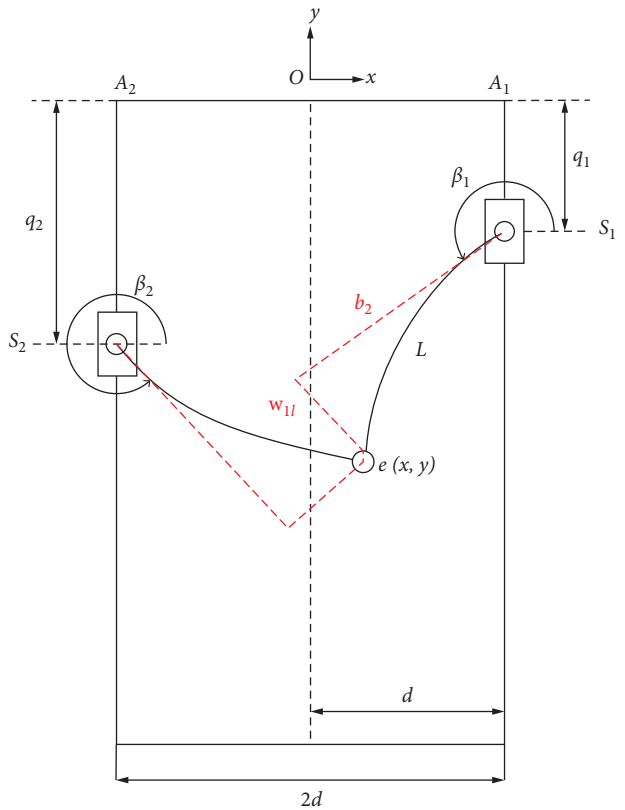

Figure 2: Coordinate system of 2-PRRRP with flexible links.

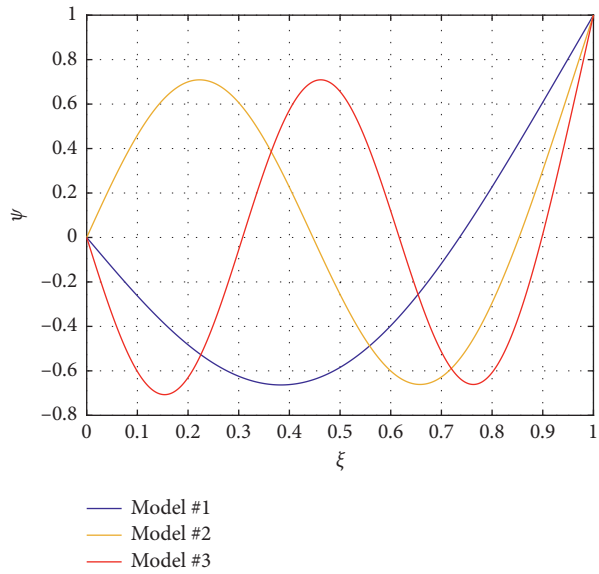

Figure 3: First three mode shapes of the flexible link.

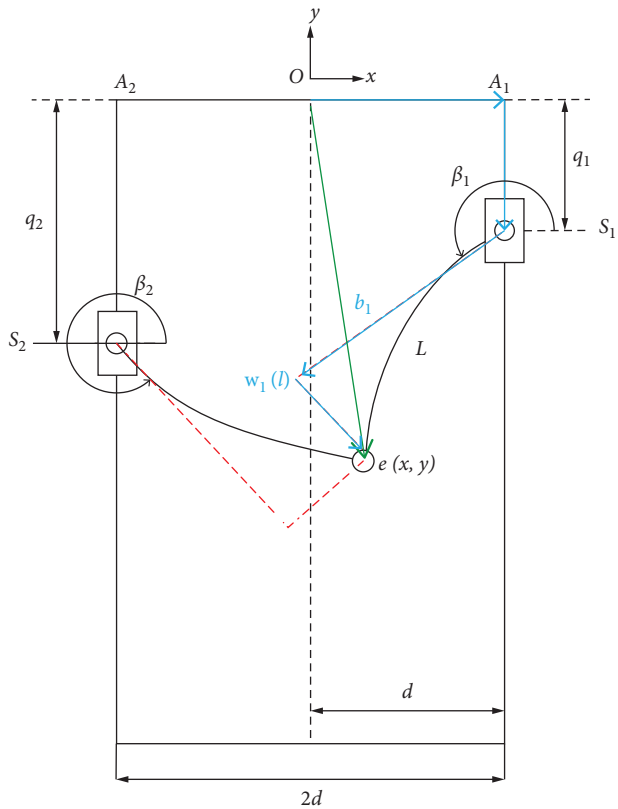

Figure 4: The closed kinematic chain of 2-PRRRP with flexible links.

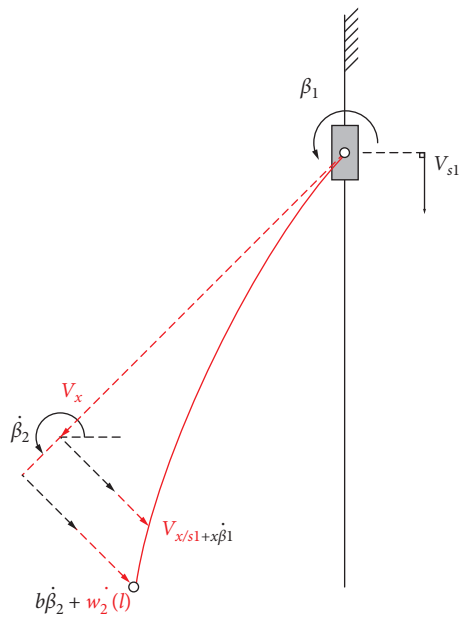

Figure 5: The kinetic energy of the flexible link.

Table 1: Dynamic parameters.

Flexible Link	Density (kg/m^3)	2770
	Young's modulus (GPa)	73
	Dimension (mm)	$360 * 30 * 5$
PZT actuator	Young's modulus (GPa)	69
	Dimension (mm)	$50 * 25 * 0.75$
Slider	Mass (kg)	0.3

Table 2: Feedback control gains.

K_P	1000 (N/m)
K_D	600 (N-s/m)
K_I	3000 (Volts-s/m)

3. Dynamic Modeling

In terms of link flexibility, the generalized coordinates are taken as follows:

$$X_{\text{flex}} = \left[\, \overline{q} \;\; \overline{\beta} \;\; \overline{X}_e \;\; \overline{\eta} \,\right]^T, \tag{7}$$

where

$$\overline{\eta} = [\;\; \eta_{11} \;\; \eta_{12} \;\; \eta_{13} \;\; \eta_{21} \;\; \eta_{22} \;\; \eta_{23} \,]^T_{6\times 1}. \tag{8}$$

Figure 4 shows the manipulator's closed kinematic chain with the flexible link deflection. Expanding equation (5), as mentioned, leads to four constraint equations, as follows:

$$\begin{cases} x_e = x_{Ai} + L\cos\beta_i - w_i(l)\sin\beta_i, \\ y_e = q_i + L\sin\beta_i + w_i(l)\cos\beta_i. \end{cases} \tag{9}$$

As shown in Figure 5, the kinematic energy is taken into account in expecting the deformation of the links:

$$T = \sum_{i=1}^{2} T_s + T_l + T_e, \tag{10}$$

where

$$\begin{cases} T_e = \dfrac{1}{2} m_e \left(\dot{x}_e^2 + \dot{y}_e^2\right), \\ T_s = \displaystyle\sum_{i=1}^{2} \frac{1}{2} m_s \dot{q}_i^2, \\ T_l = \displaystyle\sum_{i=1}^{2} \frac{1}{2} \int_0^L \rho_A v_x^2 \mathrm{d}x, \end{cases} \tag{11}$$

where ρ_A, m_s, and m_e are mass of the end-effector, mass of the sliders, and mass per length, respectively. Put the kinematic energy and the potential energy induced by link deformation for each coordinate in first-type Lagrangian equations to derive the dynamic modeling yielding the equations of motion for the flexible-link parallel manipulator:

$$\begin{bmatrix} M_{11} & M_{12} & 0 & M_{14} \\ M_{12}^T & M_{22} & 0 & M_{24} \\ 0 & 0 & M_{33} & 0 \\ M_{14}^T & M_{24}^T & 0 & M_{44} \end{bmatrix} \begin{bmatrix} \ddot{\overline{q}} \\ \ddot{\overline{\beta}} \\ \ddot{\overline{X}} \\ \ddot{\overline{\eta}} \end{bmatrix} + \begin{bmatrix} V_1 \\ V_2 \\ 0 \\ V_4 \end{bmatrix} + \begin{bmatrix} 0 & 0 & 0 & 0 \\ 0 & 0 & 0 & 0 \\ 0 & 0 & 0 & 0 \\ 0 & 0 & 0 & K \end{bmatrix} \begin{bmatrix} \overline{q} \\ \overline{\beta} \\ \overline{X} \\ \overline{\eta} \end{bmatrix} = \begin{bmatrix} F_q \\ 0 \\ F_{\text{ext}} \\ 0 \end{bmatrix} + \begin{bmatrix} J_1 \\ J_2 \\ J_3 \\ J_4 \end{bmatrix} \begin{bmatrix} \lambda_1 \\ \lambda_2 \\ \lambda_3 \\ \lambda_4 \end{bmatrix}. \tag{12}$$

Each of the components has been defined in the Appendix. Equation (12) is a differential-algebraic equation (DAE) that can be simplified by removing the Lagrangian constraint term λ_i as follows:

$$\begin{bmatrix} \overline{M}_{11}^{2\times2} & \overline{M}_{12}^{2\times6} \\ \overline{M}_{21}^{6\times2} & \overline{M}_{22}^{6\times6} \end{bmatrix} \begin{bmatrix} \ddot{\overline{X}}^{2\times1} \\ \ddot{\overline{\eta}}^{6\times1} \end{bmatrix} = \begin{bmatrix} \overline{V}_{11}^{2\times1} \\ \overline{V}_{21}^{6\times1} \end{bmatrix}. \tag{13}$$

4. Vibration Control

Structural flexibility of the links transfers undesirable vibration to the end-effector, which leads to poor tracking efficiency. When the links are flexible for linear actuators, the vibration attenuation is difficult. Thus, an active damping approach with the help of PZT is implemented. Attaching the link surface, the PZT generates a shear force that suppresses the structural vibration of the links along the length. For flexible link manipulators, the aim of the above analysis is to make the rigid mode variable follow the required trajectory or converge to a certain point while suppressing the flexible link modes. The voltage of the PZT actuators will specify the L-type approach as explained in Appendix [22]. The voltage applied to the PZT actuator can be defined as follows:

$$V_i(t) = -k_I\left[\dot{w}_i(a_2, t) - \dot{w}_i(a_1, t)\right], \tag{14}$$

where k_i represents the linear velocity feedback gain for PZT and a_1 and a_2 are the start- and end-point positions of the PZT actuators from the linear actuators, S_i, along the length. $\dot{w}_i(a_i, t)$ denotes the linear velocity of each link at a_i. The virtual work conducted by the i-th PZT actuator can be measured as follows:

$$\delta W_{\text{PZT}} = cV_i(t)\sum_{j=1}^{r}\left[\varphi_f'(a_2) - \varphi_f'(a_1)\right]\delta\eta_{ij}, \tag{15}$$

where c denotes a positive constant implying the bending moment by applying voltage. Fulfilling the PZT actuator's L-type layout is based on the position of the PZT actuator. The PZT actuator is to be installed in a region where the form function and the derivative has a similar variation trend within to achieve a stable control movement: $x \in [a_1, a_2]$.

$$(\varphi(a_2) - \varphi(a_1))(\varphi'(a_2) - \varphi'(a_1)) \geq 0. \tag{16}$$

The application of this case to higher frequency modes is limited as the fulfillment of the equation for higher frequencies is only carried out in small areas on the link.

5. Simulation Results

Two linear actuators are equipped with a simple proportional-derivative-type (PD) feedback controller system as follows:

$$f_i = -k_p(q_{di} - q_i) - k_d(\dot{q}_{di} - \dot{q}_i), \tag{17}$$

where k_p and k_d represent PD feedback gains, respectively. q_{di} and $\dot{q}_{di}$ indicate desired values for linear actuators obtained from (5).

Tables 1 and 2, respectively, include dynamic parameters and feedback control gains. Using a fourth-order, Runge–Kutta method with MATLAB software was integrated into the normal differential equations at 1 msec integration intervals.

The desired trajectory, which accelerates and decelerates smoothly, has a sinusoidal function:

$$x_e = \frac{x_f}{t_f}t - \frac{x_f}{2\pi}\sin\left(\frac{2\pi}{t_f}t\right). \tag{18}$$

The objective is that the end-effector moves 2 mm (x_f) within 10 msec (t_f).

Figure 6 illustrates the end-effector's tracking error following the desired trajectory with and without PZT actuators in the X direction. The activated profile of the PZT actuator, known as "active damping," decreases continuously as a result of the PZT actuator's damping effect, while oscillation at the initial acceleration is significant. The tracking error in active damping mode is rapidly decreased, accordingly. The label "not damping," shown in Figure 6, demonstrates that the PZT actuator is not activated. Thus, it refers to the typical features of the undamped system with flexible connections. The Y-direction movement of the end-effector, which should retain the Y position on 0 m, is also shown in Figure 7. The damping also damped the coordinate oscillations.

Also, to determine the effects of different acceleration values, the proposed path was tested using accelerations two and four times faster than the determined amount, which is exhibited in Figure 8 (i.e., the end-effector moves 4 mm and 8 mm in the same time frame in the second and third scenario). Figure 9 shows the tip deformation of every flexible link, w_i, confirming the prominent role of the PZT actuator when vibrating the links structurally as the structural vibrations are damped thoroughly after 60 msec. As reflected, the increase of acceleration puts more vibration on the manipulator, resulting in more deflection of flexible links, which were fully dampened by the active damping method in all three scenarios.

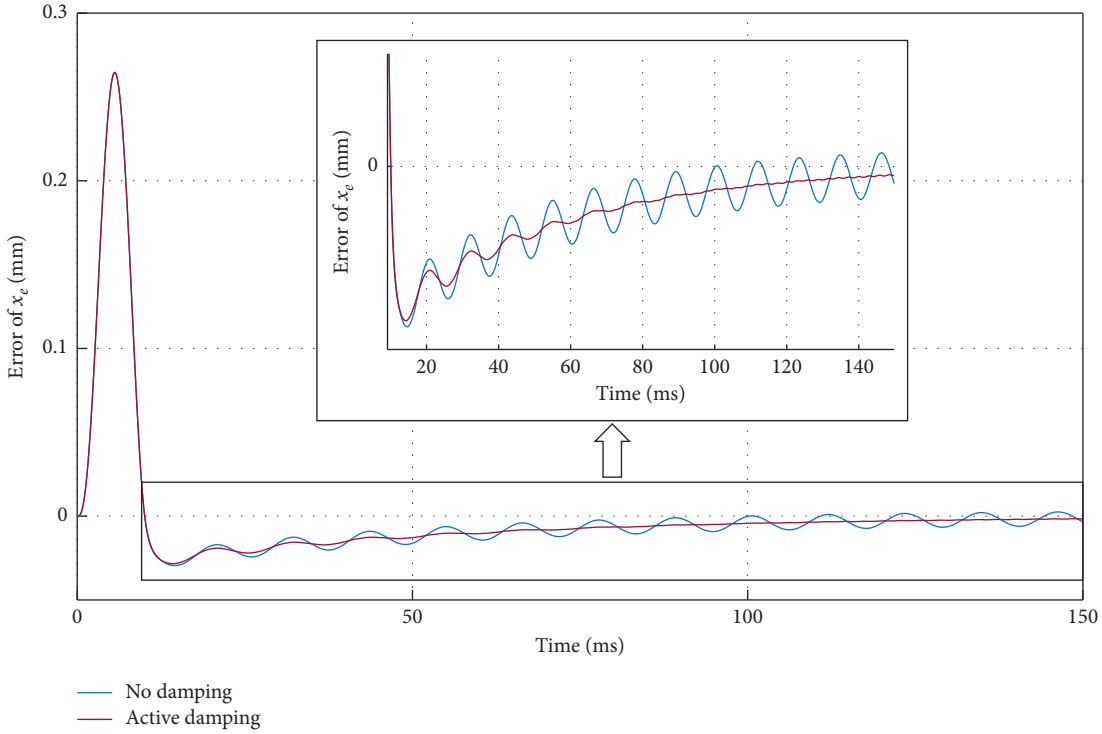

Figure 6: End effector's tracking error in X-direction between desired and actual path (blue line refers to the undamped system where red line refers to active PZT damping).

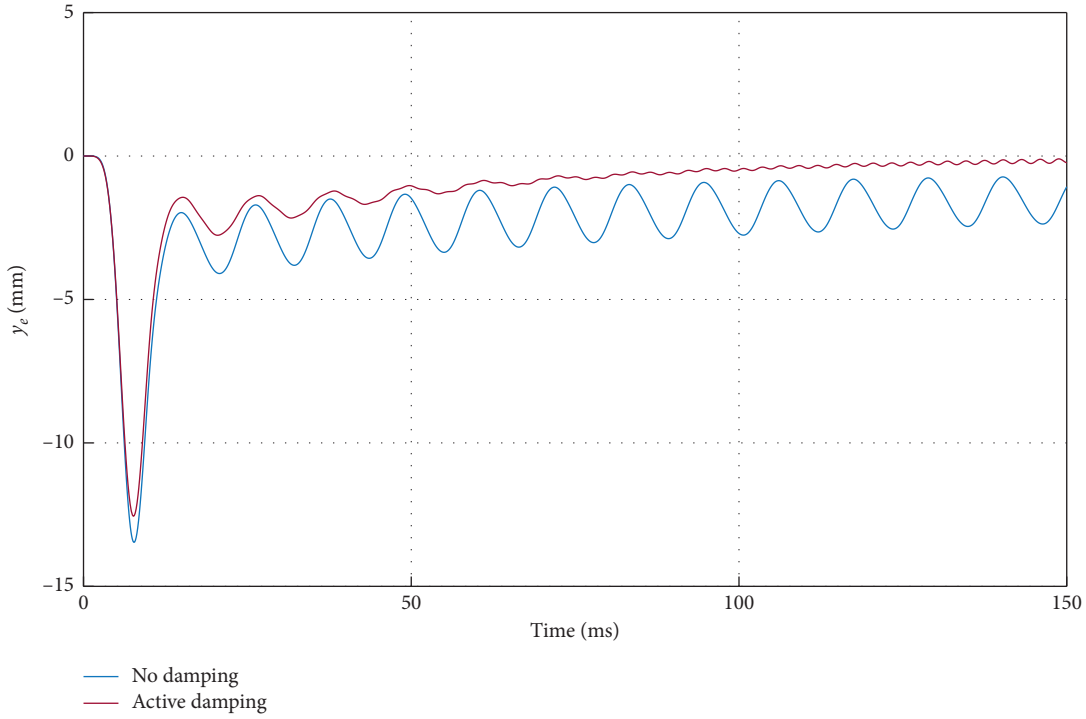

Figure 7: Y-directional movement of the end-effector.

As discussed, the dynamic model for the manipulator is studied only by the first three modes. To address this, we performed a power spectral density (PSD) analysis of the manipulator based on frequency-domain for the proposed trajectories with and without active damping; the results plotted in Figures 10–12 determine that the first mode has the

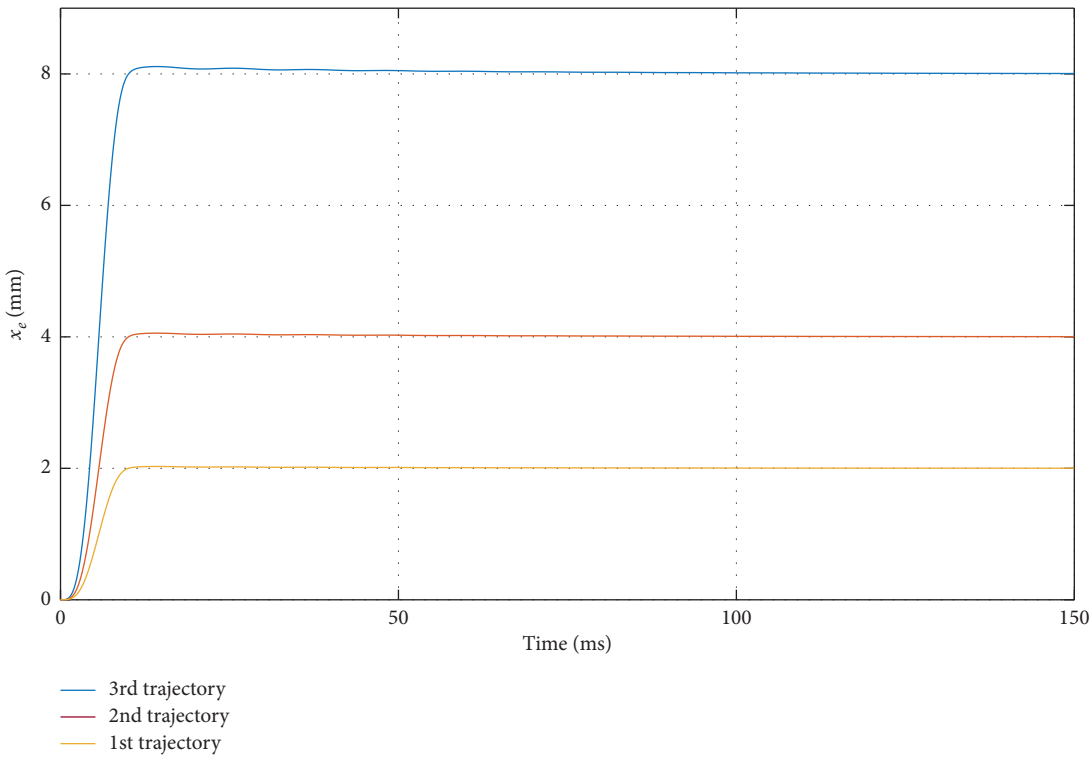

Figure 8: Accelerated trajectories (1st, 2nd, and 3rd trajectories move 2 mm, 4 mm, and 8 mm within 10 msec).

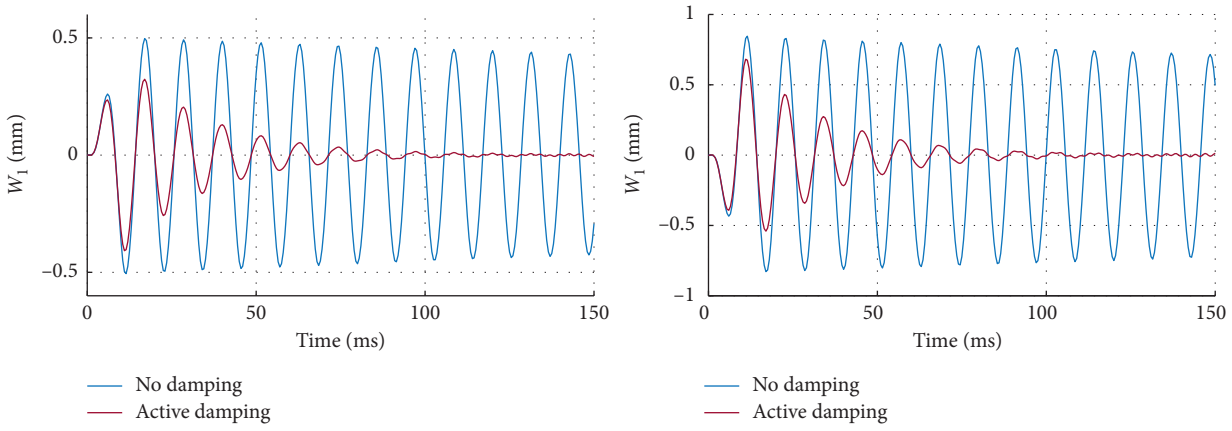

(a)

Figure 9: Continued.

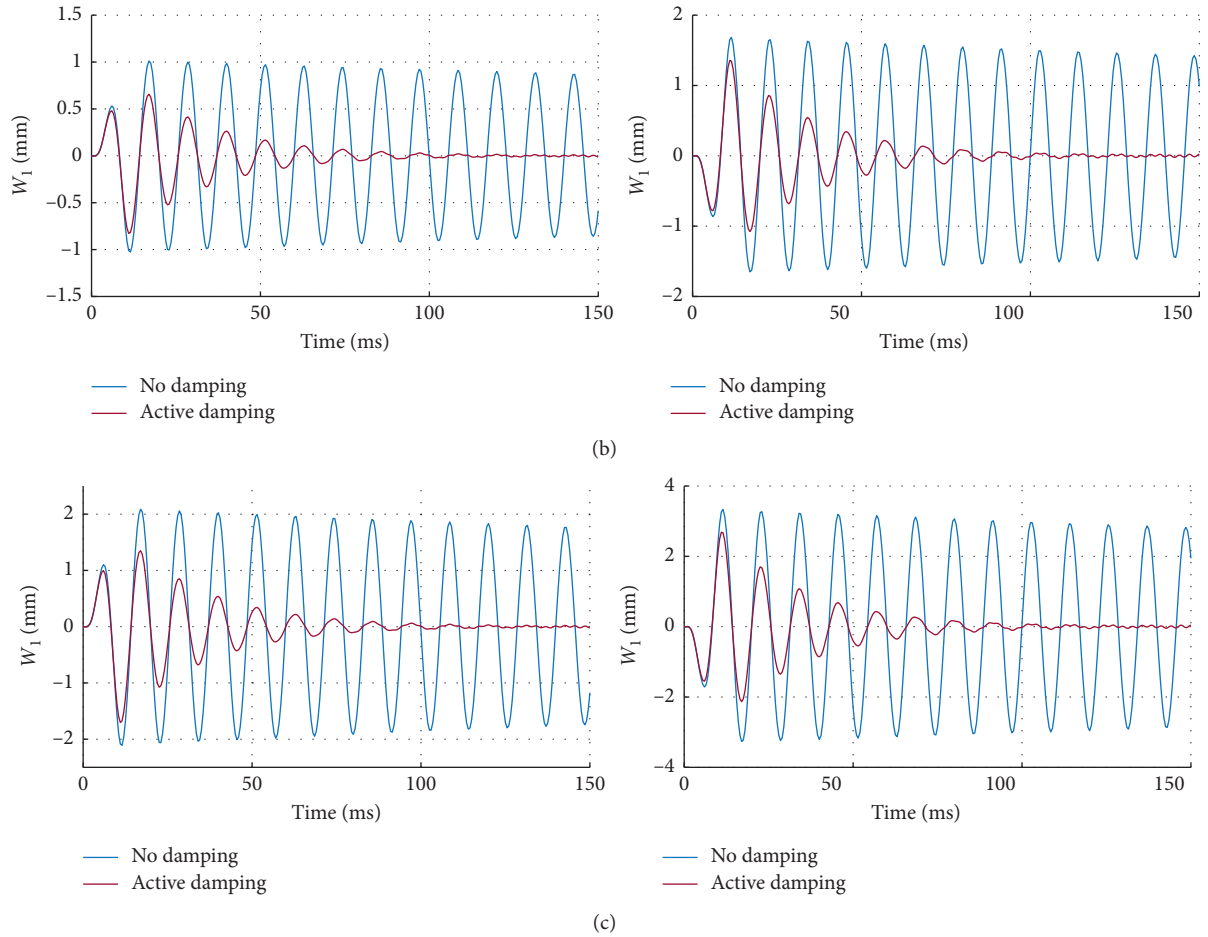

Figure 9: Flexible deformation of each links. (a) 1st trajectory. (b) 2nd trajectory. (c) 3rd trajectory.

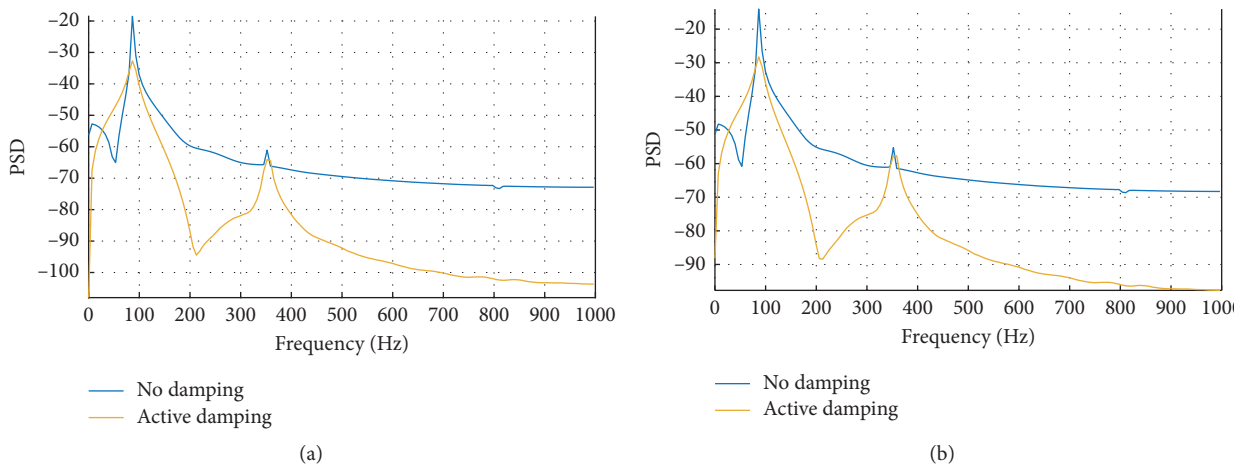

Figure 10: PSD of the first three modes of each link for the 1st trajectory. (a) 1st link. (b) 2nd link.

significant strength of the energy, while the variation at second and third modes are much weaker and had the same measures. Figures 10–12 also prove that the active damping method appropriately reduced the vibration in all given trajectories. This study's results match the research conducted by Zhang et al., in which the vibrations of an experimentally moving platform with flexible links are damped using the PZT actuators as an active control method [23]. Furthermore, well-established researches in this area obtained comprehensive damping performance by considering less than three modes of the manipulator [19, 24] and validated by experimental setups [25], which indicates the accuracy of our results.

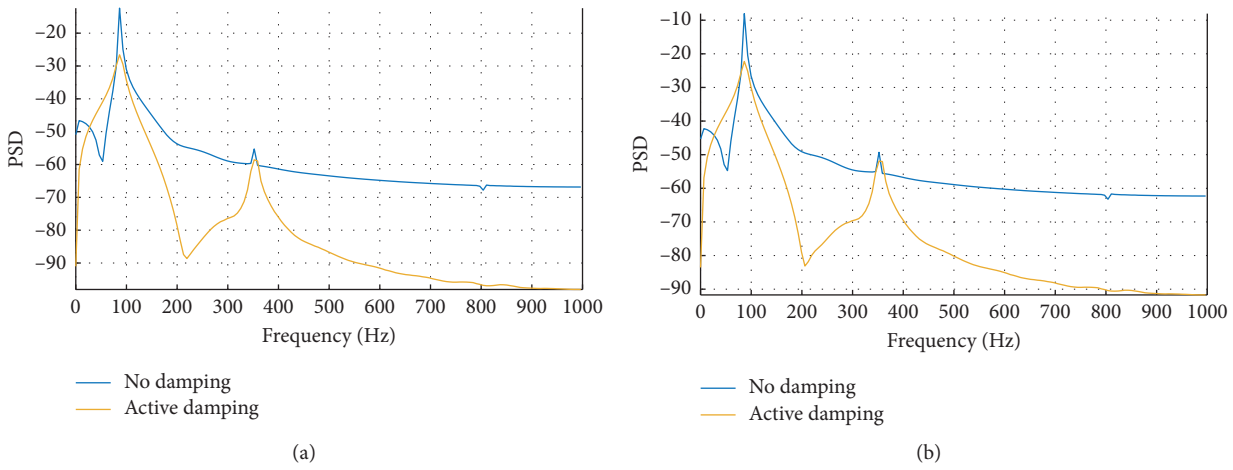

Figure 11: PSD of the first three modes of each link for the 2nd trajectory. (a) 1st link. (b) 2nd link.

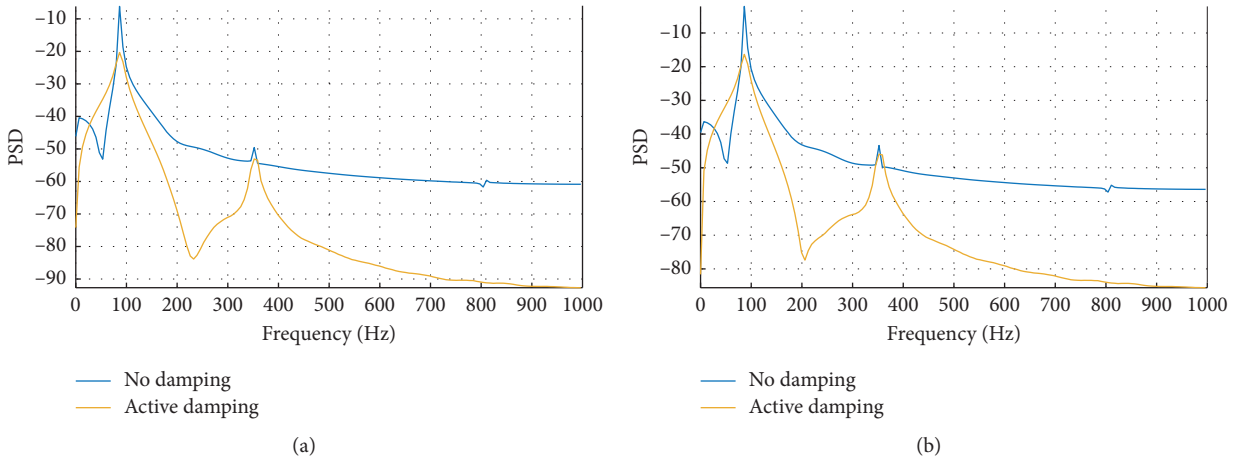

Figure 12: PSD of the first three modes of each link for the 3rd trajectory. (a) 1st link. (b) 2nd link.

6. Conclusions

2-DOF parallel manipulators containing lightweight and flexible materials are among the most discussed subjects by industrial scholars due to their extensive applications, such as pick and place tasks. In addition to the flexibility of robot links, working at high speeds makes it impossible to consider the deformation of the links as rigid. In this study, the deformation of the 2-PRRRP manipulators' links during accelerated trajectories is addressed by approaching the assumed mode method. Using the first-type Lagrangian equations, the dynamic equations of the 2-DOF flexible-link planar parallel manipulator are represented. The active damping method with the PZT actuators is considered to attenuate the structural vibration of flexible links. The piezoelectric materials can achieve a suitable damping performance with an L-type control strategy to counter structural vibration of flexible connections, which substantially reduces the time of setting of the end-effector leading to precise tracking of the trajectory. Relevant results indicate no requirement to use solid heavy links in 2-DOF parallel manipulators and spend less energy by considering them flexible.

Appendix

First-type Lagrangian equations:

$$\frac{\mathrm{d}}{\mathrm{d}t}\left(\frac{\partial T}{\partial \dot{q}_i}\right) - \frac{\partial (T - V)}{\partial q_i} = Q_i + \sum_{k=1}^{m} \lambda_k \frac{\partial \Gamma_k}{\partial q_i}. \tag{A.1}$$

Potential energy induced by link deformation:

$$U = \frac{1}{2} \sum_{i=1}^{2} E_i I_i \int_0^l \left(\frac{\partial^2 w_i(x)}{\partial x^2}\right)^2 \mathrm{d}x. \tag{A.2}$$

Equation of motion components:

$$M_{11} = (m_s + m_l)\begin{bmatrix} 1 & 0 \\ 0 & 1 \end{bmatrix},$$

$$M_{12} = \left(\frac{m_l l}{2}\right)\begin{bmatrix} c_1 & 0 \\ 0 & c_2 \end{bmatrix},$$

$$M_{22} = \left(\frac{m_l l^2}{3}\right),$$

$$M_{33} = m_p\begin{bmatrix} 1 & 0 \\ 0 & 1 \end{bmatrix},$$

$$M_{14} = \rho_A\begin{bmatrix} c_1\int\varphi_1 d\xi & c_1\int\varphi_2 d\xi & c_1\int\varphi_3 d\xi & 0 & 0 & 0 \\ 0 & 0 & 0 & c_2\int\varphi_1 d\xi & c_2\int\varphi_2 d\xi & c_2\int\varphi_3 d\xi \end{bmatrix},$$

$$M_{24} = \rho_A\begin{bmatrix} \int\varphi_1\xi d\xi & \int\varphi_2\xi d\xi & \int\varphi_3\xi d\xi & 0 & 0 & 0 \\ 0 & 0 & 0 & \int\varphi_1\xi d\xi & \int\varphi_2\xi d\xi & \int\varphi_3\xi d\xi \end{bmatrix},$$

$$M_{44} = \rho_A\begin{bmatrix} \widehat{M} & 0 \\ 0 & \widehat{M} \end{bmatrix},$$

$$\widehat{M} = \begin{bmatrix} \int\varphi_1^2 d\xi & 0 & 0 \\ 0 & \int\varphi_2^2 d\xi & 0 \\ 0 & 0 & \int\varphi_3^2 d\xi \end{bmatrix},$$

$$K = -EI\begin{bmatrix} \widehat{K} & 0 \\ 0 & \widehat{K} \end{bmatrix},$$

$$\widehat{K} = \begin{bmatrix} \int\varphi_1''^2 d\xi & 0 & 0 \\ 0 & \int\varphi_2''^2 d\xi & 0 \\ 0 & 0 & \int\varphi_3''^2 d\xi \end{bmatrix},$$

$$V_1 = \begin{bmatrix} -\rho_A\dot{\beta}_1 s_1\sum_{j=1}^{3}\dot{\eta}_{1j}\int\varphi_j d\xi - 0.5 m_l l\dot{\beta}_1^2 s_1 \\ -\rho_A\dot{\beta}_2 s_2\sum_{j=1}^{3}\dot{\eta}_{2j}\int\varphi_j d\xi - 0.5 m_l l\dot{\beta}_2^2 s_2 \end{bmatrix},$$

$$V_2 = \begin{bmatrix} \rho_A\dot{q}_1 s_1^2\sum_{j=1}^{3}\dot{\eta}_{1j}\int\varphi_j d\xi \\ \rho_A\dot{q}_2 s_2^2\sum_{j=1}^{3}\dot{\eta}_{2j}\int\varphi_j d\xi \end{bmatrix},$$

$$
\begin{aligned}
V_4 &= \begin{bmatrix}
-\rho_A \dot{q}_1 \dot{\beta}_1 s_1 \int \varphi_1 \mathrm{d}\xi \\
-\rho_A \dot{q}_1 \dot{\beta}_1 s_1 \int \varphi_2 \mathrm{d}\xi \\
-\rho_A \dot{q}_1 \dot{\beta}_1 s_1 \int \varphi_3 \mathrm{d}\xi \\
-\rho_A \dot{q}_2 \dot{\beta}_2 s_2 \int \varphi_1 \mathrm{d}\xi \\
-\rho_A \dot{q}_2 \dot{\beta}_2 s_2 \int \varphi_2 \mathrm{d}\xi \\
-\rho_A \dot{q}_2 \dot{\beta}_2 s_2 \int \varphi_3 \mathrm{d}\xi
\end{bmatrix}, \\
J_1 &= \begin{bmatrix} 1 & 1 & 0 & 0 \\ 0 & 0 & 1 & 1 \end{bmatrix}, \\
J_2 &= \begin{bmatrix} -ls_1 - w_1 c_1 & lc_1 - w_1 s_1 & 0 & 0 \\ 0 & 0 & -ls_2 - w_2 c_2 & lc_2 - w_2 s_2 \end{bmatrix}, \\
J_3 &= \begin{bmatrix} -1 & 0 & -1 & 0 \\ 0 & -1 & 0 & -1 \end{bmatrix}, \\
J_4 &= \begin{bmatrix}
-s_1 \int \varphi_1 \mathrm{d}\xi & c_1 \int \varphi_1 \mathrm{d}\xi & 0 & 0 \\
-s_1 \int \varphi_2 \mathrm{d}\xi & c_1 \int \varphi_2 \mathrm{d}\xi & 0 & 0 \\
-s_1 \int \varphi_3 \mathrm{d}\xi & c_1 \int \varphi_3 \mathrm{d}\xi & 0 & 0 \\
0 & 0 & -s_2 \int \varphi_1 \mathrm{d}\xi & c_2 \int \varphi_1 \mathrm{d}\xi \\
0 & 0 & -s_2 \int \varphi_2 \mathrm{d}\xi & c_2 \int \varphi_2 \mathrm{d}\xi \\
0 & 0 & -s_3 \int \varphi_3 \mathrm{d}\xi & c_2 \int \varphi_3 \mathrm{d}\xi
\end{bmatrix}, \\
F_q &= \begin{bmatrix} F_1 \\ F_2 \end{bmatrix}, \\
F_{\text{ext}} &= \begin{bmatrix} F_x \\ F_y \end{bmatrix},
\end{aligned}
\tag{A.3}
$$

where $c_i = \cos(\beta_i), s_i = \sin(\beta_i)$.

Voltage generated by PZT sensor:

$$
\begin{aligned}
V_s &= k_s \varepsilon \\
&= k_s \frac{\sigma}{E} \\
&= k_s \frac{MC/I}{E} \\
&= k_s \left(\frac{\partial^2 w(x,t)}{\partial x^2} \right).
\end{aligned}
\tag{A.4}
$$

Using strain rate feedback,

$$
\begin{aligned}
V_i(t) &= -k' \dot{\varepsilon} \\
&= -k' \frac{\dot{V}_s}{k_s} \\
&= -k_I \dot{w},
\end{aligned}
\tag{A.5}
$$

where $-k'$ is control gain applied to the PZT actuator.

Data Availability

No data were used to support this study.

Conflicts of Interest

The authors declare no conflicts of interest.

References

[1] S. K. Dwivedy and P. Eberhard, "Dynamic analysis of flexible manipulators, a literature review," *Mechanism and Machine Theory*, vol. 41, no. 7, pp. 749–777, 2006.

[2] J. M. San Martins, Z. Mohamed, M. O. Tokhi, J. Sá da Costa, and M. A. Botto, "Approaches for dynamic modelling of flexible manipulator systems," *IEE Proceedings - Control Theory and Applications*, vol. 150, no. 4, pp. 401–411, 2003.

[3] M. Benosman and G. L. Vey, "Control of flexible manipulators: a survey," *Robotica*, vol. 22, no. 5, pp. 533–545, 2004.

[4] W. Z. Gebrehiwot, "Design and control of a five bar linkage parallel manipulator with flexible arms," MSc thesis, Politecnico Di Milano, Milan, Italy, 2009.

[5] H. Asada, Z. D. Ma, and H. Tokumaru, "Inverse dynamics of flexible robot arms: modeling and computation for trajectory control," *Journal of Dynamic Systems, Measurement, and Control*, vol. 112, no. 2, pp. 177–185, 1990.

[6] F. Wang and Y. Gao, *Advanced Studies of Flexible Robotic Manipulators: Modeling, Design, Control and Applications*, World Scientific Publishing, Singapore, 2003.

[7] X. J. Liu, J. Wang, and G. Pritschow, "On the optimal kinematic design of the PRRRP 2-DoF parallel mechanism," *Mechanism and Machine Theory*, vol. 41, no. 9, pp. 1111–1130, 2006.

[8] G. Piras, W. L. Cleghorn, and J. K. Mills, "Dynamic finite-element analysis of a planar high speed, high-precision parallel manipulator with flexible links," *Mechanism and Machine Theory*, vol. 40, no. 7, pp. 849–862, 2005.

[9] M. O. Tokhi, Z. Mohamed, and M. H. Shaheed, "Dynamic characterisation of a flexible manipulator system," *Robotica*, vol. 19, no. 5, pp. 571–580, 2001.

[10] M. O. Tokhi, Z. Mohamed, and A. K. M. Azad, "Finite difference and finite element approaches to dynamic modelling of a flexible manipulator," *Journal of Systems and Control Engineering*, vol. 211, no. 2, pp. 145–156, 1997.

[11] G. G. Hasting and W. J. Book, "A linear dynamic model for flexible robot manipulators," *IEEE Control Systems Magazine*, vol. 7, no. 1, pp. 61–64, 1987.

[12] A. K. M. Azad, *Analysis and Design of Control Mechanism for Flexible Manipulator Systems*, PhD Thesis, The University of Sheffield, Sheffield, UK, 1994.

[13] Z. Zhou, J. Xi, and C. K. Mechefske, "Modeling of a fully flexible 3PRS manipulator for vibration analysis," *Journal of Mechanical Design*, vol. 128, no. 2, pp. 403–412, 2006.

[14] X. Zhang, J. K. Mills, and W. L. Cleghorn, "Study on the effect of elastic deformations on rigid body motions of a 3-PRR flexible parallel manipulator," in *IEEE International Conference on Mechatronics and Automation*, pp. 1805–1810, Harbin, China, August 2007.

[15] J. Wu, T. Li, X. Liu, and L. Wang, "Optimal kinematic design of a 2-DOF planar parallel manipulator," *Tsinghua Science and Technology*, vol. 12, no. 3, pp. 269–275, 2007.

[16] B. Kang and J. K. Mills, "Dynamic modeling of structurally-flexible planar parallel manipulator," *Robotica*, vol. 20, no. 3, pp. 329–339, 2002.

[17] K. S. Fu, R. C. Gonzalez, and G. S. G. Lee, *Robotics: Control, Sensing, Vision and Intelligence*, McGraw-Hill, New York, NY, USA, 1987.

[18] M. W. Spong and M. Vidyasagar, *Robot Dynamics and Control*, J. Wiley, Chichester, UK, 1989.

[19] B. Kang and J. K. Mills, "Study on piezoelectric actuators in vibration control of a planar parallel manipulator," in *IEEE/ASME International Conference on Advanced Intelligent Mechatronics*, pp. 1268–1273, 2003.

[20] M. O. Tokhi and A. K. M. Azad, *Flexible Robot Manipulators: Modelling, Simulation and Control*, IET, London, UK, 2008.

[21] M. H. Korayem and H. N. Rahimi, "Nonlinear dynamic analysis for elastic robotic arms," *Frontiers of Mechanical Engineering*, vol. 6, no. 2, pp. 219–228, 2011.

[22] D. San Sun and J. K. Mills, "PZT actuator placement for structural vibration damping of high speed manufacturing equipment," in *Proceedings of the American Control Conference*, pp. 1107–1111, San Diego, CA, USA, June 1999.

[23] X. Zhang, J. K. Mills, and W. L. Cleghorn, "Experimental implementation on vibration mode control of a moving 3-PRR flexible parallel manipulator with multiple PZT transducers," *Journal of Vibration and Control*, vol. 16, no. 13, pp. 2035–2054, 2010.

[24] X. Zhang, J. K. Mills, and W. L. Cleghorn, "Vibration control of elastodynamic response of a 3-PRR flexible parallel manipulator using PZT transducers," *Robotica*, vol. 26, no. 5, pp. 655–665, 2008.

[25] X. Zhang, J. K. Mills, and W. L. Cleghorn, "Dynamic modeling and experimental validation of a 3-PRR parallel manipulator with flexible intermediate links," *Journal of Intelligent and Robotic Systems*, vol. 50, no. 4, pp. 323–340, 2007.